COMMENTS ON DIFFRACTION PROCESSES AND TOTAL CROSS SECTIONS

Douglas R.O. MORRISON
CERN, Geneva

Abstract : Some controversial aspects of diffraction dissociation are discussed in the light of some recent results. Evidence is presented that the A_1, A_3, Q and L mass enhancements are not single resonant states and that an $N^*(1400)$ is not required. It is suggested that the cross section for diffraction dissociation is almost equal to that for diffraction elastic scattering and both are slowly rising as does the total inelastic cross section, i.e., as $s^{+0.04}$ or $(\log s)^{+0.4}$. The Reggeon exchange part of pp elastic scattering then falls as s^1.

Résumé : Quelques aspects controversiels de la dissociation diffractive sont discutés à la lumière de quelques résultats récents. On montre que A_1, A_3, Q et L ne sont pas des états résonants individuels et que le N^* (1400) n'est pas requis. On suggère que la section efficace de la dissociation diffractive est presque égale à la section efficace élastique et que les deux augmentent légèrement de la même manière que la section totale inélastique, à savoir comme $s^{+0.04}$ ou $(\log s)^{+0.4}$. La partie de pp élastique due à l'échange de Reggeons tombe alors comme s^1.

INTRODUCTION

In this paper we will concentrate on some more controversial aspects of diffraction processes and the relation to total and inelastic cross sections. More complete reviews of diffraction have recently been given by Leith [1] in last year's Rencontre de Moriond and in ref. 2. Many of the ideas presented here were previously given in refs. 2 and 3.

The subjects that we would like to discuss are :

1. Are the A_1, A_3, Q, L,... resonances ?
2. Does the $N^*(1400)$ exist ?
3. The ratio of the cross section for inelastic diffraction to that for elastic diffraction.
4. Relationship between total, inelastic, and diffractive cross sections.

1. ARE A_1, A_3, Q, L,... RESONANCES ?

Recently considerable progress in understanding inelastic diffractive processes has come from Partial Wave Analyses, P.W.A. using the Ascoli program [4] whose assumptions have been discussed by Hansen et al.,[5]. The method has been applied [6,7,8] to the pion reactions

$$\pi^{\pm} p \rightarrow (\pi^{-}\pi^{+}\pi^{-})^{\pm} p \qquad (1)$$

where there are two large mass enhancements, the A_1 and the A_3, and recently the program has been modified to study [9] the K^-p reactions

$$K^{-} p \rightarrow (K^{-}\pi^{+}\pi^{-}) p \qquad (2)$$

where these are two similar large mass enhancements the Q and the L.

The Aachen-Berlin-CERN-London-Vienna Collaboration [9] show in fig. 1a that 95 % of the reaction (2) proceeds by natural parity exchange i.e., $J^P = 0^+, 1^-, 2^+, \ldots$, this is in agreement with the assumption that the main process is diffraction dissociation taken to be 0^+ exchange. Further they show in fig. 1b that the $(K\pi\pi)$ system produced is mainly (88 %) in the unnatural spin-parity series $0^-, 1^+, 2^-, 3^+, \ldots$ This is consistent with the suggestion [10] that states are suppressed if they do not obey the spin-parity rule,

$$P_f = P_i (-1)^{\Delta J} \qquad (3)$$

where P_i and P_f are the initial and find parities and ΔJ is the change in spin. Most of the remaining 12 % produced is the $K^*(1420)$ with $J^P = 2^+$. The situation in reaction (1) is similar; the CERN-Serpukhov Collaboration find that at 40 GeV/c the A_2 cross section is almost an order of magnitude smaller than that of the A_1.

The separation of (3π) system into various J^P states at 40 GeV/c [7] is shown in fig. 2 and a similar separation for $(K\pi\pi)^-$ states at 10 and 16 GeV/c [9] are given in fig.3. It maybe seen that the detailed J^P structure is similar in the two cases with 1^+S dominating and 0^- important at low masses while at higher masses 2^-S gives a significant peak (near the A_3 and L^- mesons respectively). At still higher masses 3^+ gives significant contributions. It is frequently reported that the A_1 and Q are 1^+ enhancements or resonances while the A_3 and L are 2^- enhancements or resonances. This has been tested by the ABCLV Collaboration [9] in fig.4. In the top figure the total number of events is plotted and also the numbers of events in 1^+S states decaying into $K\rho$ and $K^*\pi$ and 2^-S states decaying into $(K^*1420\ \pi)$ and Kf In fig. 4b, these 1^+S and 2^-S contributions have been subtracted from the total and the remainder is plotted, it may be seen that this remainder is significant and has a two humped structure. It is concluded that the Q and L cannot be considered as single resonant states.

Another piece of evidence on this subject of resonance or not, are the values of the relative phase ϕ between the state of interest and other states. For the $(3\pi)^-$ system produced at 40 GeV/c [7], these phases are plotted in fig. 5 as functions of mass for the "A_1", A_2 and "A_3". It may be seen that for the 2^+D wave i.e., the A_2, the angle ϕ varies rapidly with mass as it is expected for the well established A_2 resonance (we consider it to be well established as it is observed in reactions with other types of exchange, e.g., change exchange). On the other hand for the "A_1" and "A_3", the angle Ø does not vary across the mass enhancement showing that these are not resonances *.

2. DOES THE N^*(1400) EXIST ?

In single arm counter experiments the missing mass MM is measured for reactions such as

$$\pi^- + p \rightarrow p + MM \qquad (4)$$

A typical result for π^-p reactions at small $|t|$- values is shown in fig.5. The data are interpreted as the production of N^* isobars as in the reaction.

$$\pi^- + p \rightarrow p + N^* \qquad (5)$$

plus a non-resonant background, the marked peaks as seen in fig.6 indicating the N^* isobars to be considered. To interpret the data it was found necessary to introduce a new isobar, the N^*(1400) which has not been observed in phase shift analyses of formation experiments. At very small $|t|$ values, the experimentally observed peak is near 1350 MeV, and as the $|t|$ value increases the peak moves towards 1500 MeV. However, by employing several resonances and by a judicious choice of non-resonant background, the new isobar mass is kept near 1400 MeV for each t- interval. However, it is difficult to explain why this non-resonant background is so large (greater than the resonant cross section) and why no N^*(1400) is found by phase shift analysis.

---

*) Recently an analysis of $(3\pi)^+$ system produced in the reaction $\pi^+p \rightarrow (3\pi)^+p$ at 13 GeV/c [8] has indicated some variation of Ø over the A_3 mass region. However, unpublished work [10] with π^+p reactions at 8,16 and 23 GeV/c finds no such variation.

Bubble chamber experiments have the advantage that the total number of produced particles can often be identified and hence the missing mass spectrum can be separated into the different multiplicity channels. An example of this is shown in fig. 7 where in a) the $N\pi$ (baryon-pion) mass spectrum shows a broad enhancement at low masses and a sharp fall off above 1690 MeV and in b) the $(N\pi\pi)$ mass spectrum shows two peaks, at 1470 and 1710 MeV respectively. In fig. 7c, the summed spectrum shows peaks at the $\Delta(1236)$, at 1470 and 1690 MeV, but no peak near 1400 MeV, note that in the bubble chamber experiment all t- intervals are added together unlike fig. 6. The baryon-pion mass spectrum has been further analysed by isospin analysis [11] by which the $I = \frac{3}{2}$, $N^*(1236)$ can be separated off. It is found that the $I = \frac{1}{2}$ $(N\pi)$ system has a broad enhancement with a maximum near 1350 MeV and a peak near 1690 MeV. Thus the bubble chamber results suggest that there is no need to have a $N^*(1400)$ which is moderately narrow ($\Gamma \sim 200$ MeV). A possible interpretation [12] of the data is that there are two processes

a) production of resonant isobars which are also found in phase shift analyses $\Delta(1236)$ and $N^*(1690)$

b) broad enhancements produced by diffraction dissociation. These would occur both in the $(N\pi)$ and $(N\pi\pi)$ mass spectra, but because of phase space and of the decay mechanism of the $(N\pi\pi)$ system, the peak value, width and t-dependence will be different in the $N\pi$ and $(N\pi\pi)$ cases. This would be the explanation of the hump in the missing mass spectrum which shifts its peak value with the t interval.

Thus, in conclusion the experimented evidence does not require an $N^*(1400)$ and the data are more naturally interpreted without employing an $N^*(1400)$.

3. INELASTIC DIFFRACTION AND ELASTIC DIFFRACTION CROSS SECTIONS

In this chapter we discuss the cross sections of inelastic diffraction and of elastic diffraction processes. We start with the work of the ABCLV Collaboration [13] who interpreted K^-p reactions as being the sum of three processes as illustrated in fig. 8 below

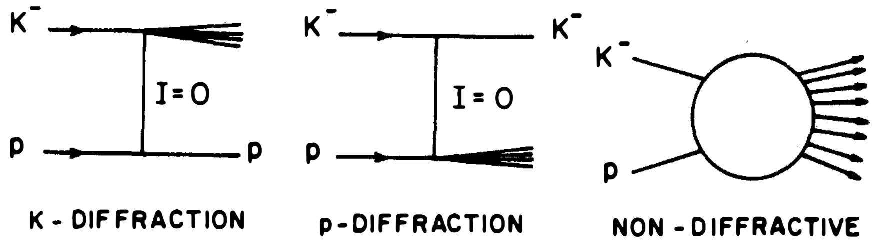

Fig. 8

The total cross sections for these three processes are σ_{KD}, σ_{pD} and σ_M, respectively (M ≡ non-diffractive, e.g., multiperipheral). If the cross section for any total or "true" multiplicity, n, is σ^n, then,

$$\sigma^n = \sigma^n_{KD} + \sigma^n_{pD} + \sigma^n_M \tag{6}$$

The "true" multiplicity was derived from the measured channel cross sections (4C and 1C fits) and using statistical isospin weights to derive ratios between the different reactions of the same multiplicity. This is illustrated in table 1 below for the case of n = 4

TABLE 1

Statistical isospin weights and measured cross sections for 4-body K^-p reactions at 10 GeV/c

CHANNEL	MEASURED CROSS SECTION mb	COEFFICIENTS		
		K DIFF.	p DIFF.	NON-DIFF.
$\bar{K}^o n\pi^+\pi^-$	0.30 ± 0.02	0	0	21/90
$\bar{K}^o p\pi^-\pi^o$	0.62 ± 0.03	2/6	0	17/90
$K^-p\pi^+\pi^-$	0.87 ± 0.02	3/6	3/6	21/90
$K^-p\pi^o\pi^o$	NOT MEASURED	1/6	1/6	7/90
$K^-n\pi^+\pi^o$	NOT MEASURED	0	2/6	17/90
$\bar{K}^o n\pi^o\pi^o$	NOT MEASURED	0	0	7/90

For each multiplicity there are 3 unknown σ^n_{KD}, σ^n_{pD}, and σ^n_M but K^-p reactions have the advantage that for each multiplicity three channel cross sections can be measured in a bubble chamber experiment.

Several interesting results are obtained, such as that the cross section for the diffractive dissociation of K into (Kπ) is consistent with zero, but the most important result is that adding all multiplicities together, the cross section for kaon dissociation is approximately equal to that for proton dissociation that is

$$\sigma_{KD}(K^-p) = \sigma_{pD}(K^-p) \tag{7}$$

A similar result has been derived from π^-p reactions at 205 GeV/c [14]

$$\sigma_{\pi D}(\pi^-p) = \sigma_{pD}(\pi^-p) \tag{8}$$

The total multiplicity distributions of proton, kaon or pion diffraction dissociation are different, but their total cross section can be equal as illustrated in fig. 9 below

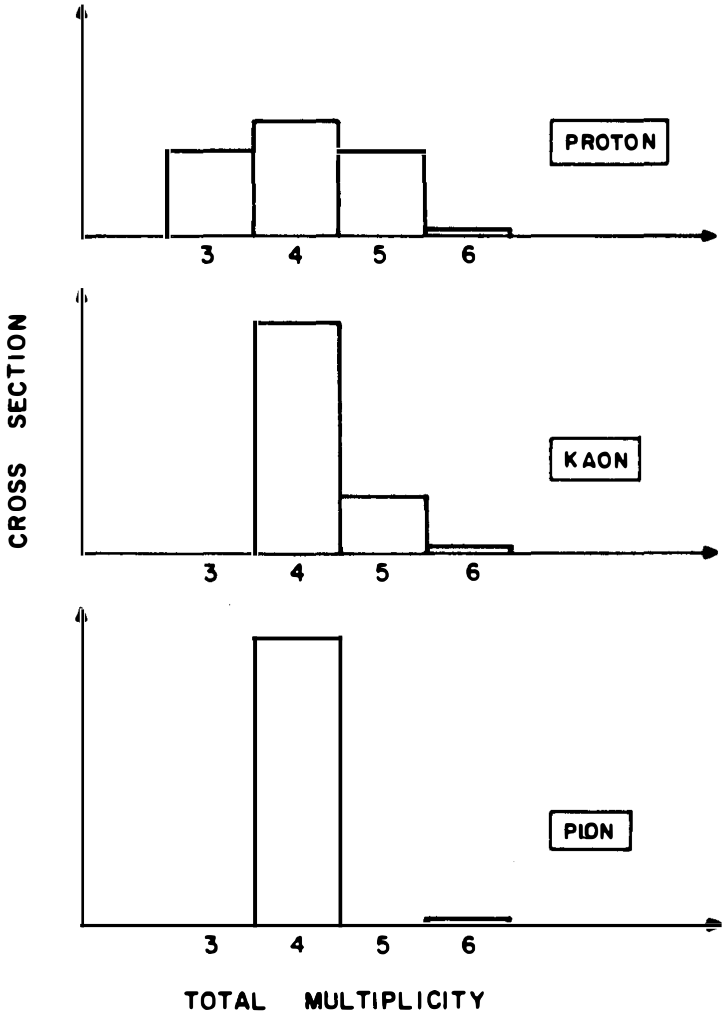

Fig. 9

If we assume factorization, then some important results on the ratio of diffraction dissociation to elastic diffraction cross sections can be derived [2] . For kaon and proton diffraction we assume the coupling constants at the vertices as indicated in fig. 10 below, where P is the Pomeron.

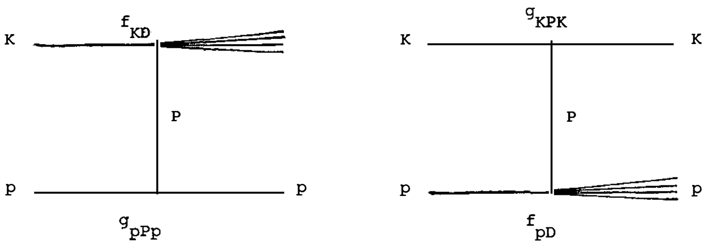

Fig. 10

Then from Eq. (7)

$$\sigma_{KD}(K^-p) = f^2_{KD} \cdot g^2_{pPp} = f^2_{pD} \cdot g^2_{KPK} = \sigma_{pD}(K^-p)$$

$$\frac{\sigma_{KD}(K^-p)}{\sigma_{EL}(Kp)} = \frac{\sigma_{pD}(Kp)}{\sigma_{EL}(Kp)} = \frac{f^2_{pD} \cdot g^2_{KPK}}{g^2_{pPp} \cdot g^2_{KPK}} \cdot \frac{g^2_{pPp}}{g^2_{pPp}} \tag{9}$$

$$= \frac{\sigma_{pD}(pp)}{\sigma_{EL}(pp)} = \frac{\sigma_{\pi D}(\pi p)}{\sigma_{EL}(\pi p)} = k_D$$

Thus we have derived a ratio between inelastic diffractive and elastic cross sections for Kp, πp and pp reactions and this ratio is the same in each case, k_D say. Then adding both vertices, the total single diffraction dissociation, SDD, cross section is given by

$$\frac{\sigma(\text{total SDD})}{\sigma_{EL}} = 2k_D \tag{10}$$

If DDD is double diffraction dissociation (i.e., diffraction at both vertices simultaneously) then by factorization it can be shown that

$$\frac{\sigma(\mathrm{DDD})}{\sigma_{EL}} = k_D^2 \tag{11}$$

Then the total diffraction dissociation cross section (single plus double) is given by

$$\frac{\sigma(\mathrm{total\ DD})}{\sigma_{EL}} = 2k_D + k_D^2 \tag{12}$$

From many experimental results, one can take $k_D \approx 0.4$ so that the total inelastic diffraction dissociation cross section is almost equal to the elastic diffractive cross section.

4. RELATIONSHIP BETWEEN TOTAL, ELASTIC AND DIFFRACTIVE CROSS SECTIONS

That the total cross section, σ_T, increases with energy over the ISR range [15,16,17] is now confirmed by the USA-USSR Collaboration [18] results on the ratio of the real to imaginary parts of the forward scattering amplitude. This is a very important result; but it may be asked if the total cross section is the most sensitive measurement, we would like to suggest [3] that the inelastic cross section σ_{inel} may be a more direct measurement of essential parameters. The reasoning is as follows : σ_T is the sum of two parts, the inelastic and the elastic cross sections

$$\sigma_T = \sigma_{inel} + \sigma_{el} \tag{13}$$

At very high energies we consider the elastic part to consist only of diffractive effects, the Reggeon contributions having fallen to effectively zero. Now diffractive elastic scattering may be considered as the shadow of the inelastic scattering. What we are interested in primarily is the actual interaction, rather than its shadow. For example consider the case of Mr. Smith walking over the hill towards us on a sunny day, we say "Here is Mr. Smith", not "Here is Mr. Smith and his shadow". The latter statement is quite correct and the shadow gives us a lot of information, but Mr. Smith is our basic concern.

In fig. 11, the total, inelastic and elastic cross sections are shown for proton-proton reactions. The startling feature is that the inelastic cross section rises monotonically whereas σ_T and σ_{el} have a hump near threshold, decrease up to $\sim$ 100 GeV/c and then rise slowly. Over the very wide range from 6 to 1500 GeV/c, σ_{inel} has been found [3] to give a good fit to the expression s^{α} with $\alpha = + 0.04$. A reasonable fit to the expression $(\log s)^N$ is obtained with N = 0.2 over this range, while over the range 100 to 1500 GeV/c, N = 0.4 gives the best fit*.

---

*) It may be noted that these values of the exponent N, are much lower than the value of 1.8 ± 0.4 suggested from the fitting of $\sigma_T = \sigma_o + A(\log s)^N$ this seems to us to be a poor fit to make as σ_T does not decrease below σ_o.

Our picture of high energy collisions is that corresponding to the size of the two incident particles, there is a certain inelastic cross section. Because this inelastic cross section exists, there must be diffraction effects. These diffraction effects appear in two ways : elastic diffraction and inelastic diffraction. The consequence of there being inelastic diffraction, means that the inelastic cross section is increased and there is more diffraction i.e.

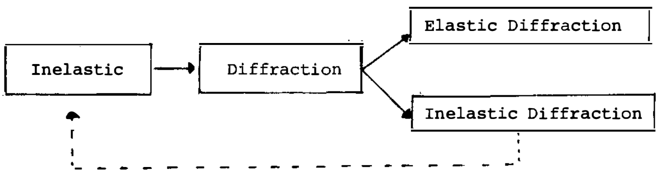

(14)

The elastic cross section is considered to consist of two parts, one diffractive (often called Pomeron exchange) and the other produced by Reggeon exchange (e.g., π, ρ, ω,... exchange), see fig. 12

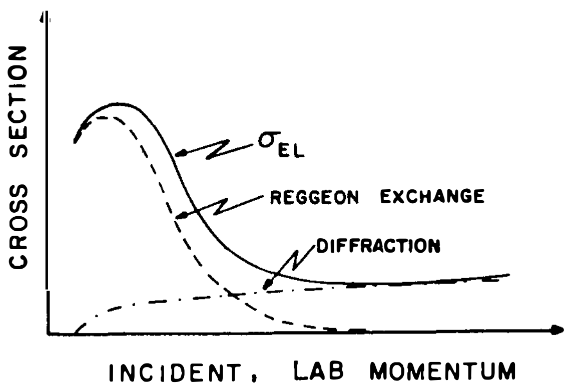

Fig. 12

At low energies Reggeon exchange is dominant and this accounts for the hump in the total elastic cross section σ_T at $\approx$ 1 GeV/c but this contribution decreases with energy and at high energies only the diffractive contribution is important. We assume that the "shadow" is a constant fraction of the total inelastic cross section, σ_{inel}. Assuming this fraction is that given at 1500 GeV/c, we can then derive σ_{el}(diffr.) at lower energies since, σ_{inel} is known. This is shown in fig. 13. The Reggeon exchange cross section, σ_{el} (Reggeon) is obtained by subtracting σ_{el}(diffr.) from σ_{el}. It is then found that the fall-off of the Reggeon exchange cross section is as s^1, and this exponent of one is about what would be expected from a mixture of $\pi, \rho, \omega, \ldots$ exchange.

The inelastic diffractive cross section σ_{inel}(diffr.) is assumed to be a constant fraction of σ_{inel} and as explained in chapter 3, to be almost equal to the diffractive elastic cross section, that is

$$\frac{\sigma_{inel}(\text{diffr.})}{\sigma_{inel}} = \text{constant} \approx \frac{\sigma_{inel}(\text{diffr.})}{\sigma_{inel}} \qquad (15)$$

The non-diffractive inelastic cross section is obtained by subtracting σ_{inel}(diffr.) from σ_{inel}. This is what we are searching for (it is equivalent to our Mr. Smith) and on this picture it will have the same energy dependence as σ_{inel}, i.e., $s^{+0.04}$ or $(\log s)^{+0.4}$. Cross section variations that occur below $\approx$ 100 GeV/c may be considered as threshold effects. A fuller discussion is given in chapter II of ref. 2.

REFERENCES

[1] D.W.G.S. Leith, 8th Rencontre de Moriond, and SLAC-PUB- 1263 (1973).

[2] D.R.O. Morrison, Proc. of 5th Hawaii Topical Conf. August 1973 and CERN/D.Ph.II/Phys. 73-46.

[3] D.R.O. Morrison, Proc. of Royal Society A 335 (1973) 461-483.

[4] G. Ascoli et al., Phys.Rev. B7 (1973) 669.

[5] J.D. Hansen, G.T. Jones, G. Otter and G. Rudolph, CERN/D.Ph.II/Phys. 73-37.

[6] Illinois, U. Kruse et al., submitted to Batavia Conf. (1972).

[7] CERN-Serpukhov Collaboration, Yu. M. Antipov, Nuclear Phys. B63 (1973) 153.

[8] Purdue, G. Thompson et al., Phys.Rev. Letters 32 (1974) 331.

[9] Aachen-Berlin-CERN-London-Vienna Collaboration, M. Deutschmann et al., to be published in Phys.Letters and CERN/D.Ph.II/PHYS 74-1

[10] Aachen-Berlin-Bonn-CERN-Heidelberg Collaboration, (unpublished).

[11] e.g., Aachen-Bonn-CERN-Heidelberg Collaboration, P. Bosetti et al., Nuclear Phys. B62 (1973) 1.

[12] D.R.O. Morrison, Rapporteur's talk, Kiev Conf. on High Energy Physics and CERN/D.Ph.II/PHYS. 71-10 and 70-6.

[13] Aachen-Berlin-CERN-London-Vienna Collaboration, M. Deutschmann et al., Nuclear Phys. B70 (1974) 237.

[14] Berkeley-NAL, G.S. Abrams et al., Berkeley report LBL-2112 (1973).

[15] CERN-Rome, U. Amaldi et al., Phys. Letters B43 (1973) 231.

[16] Pisa-Stony Brook, S.R. Amendolia et al., Phys.Letters B44 (1974) 119.

[17] CERN-Rome, U. Amaldi et al., Phys.Letters B44 (1973) 112.

[18] Moscow-NAL-Rockefeller-Rochester Collaboration, V. Bartenev et al., Phys. Rev.Letters 31 (1973) 1367.

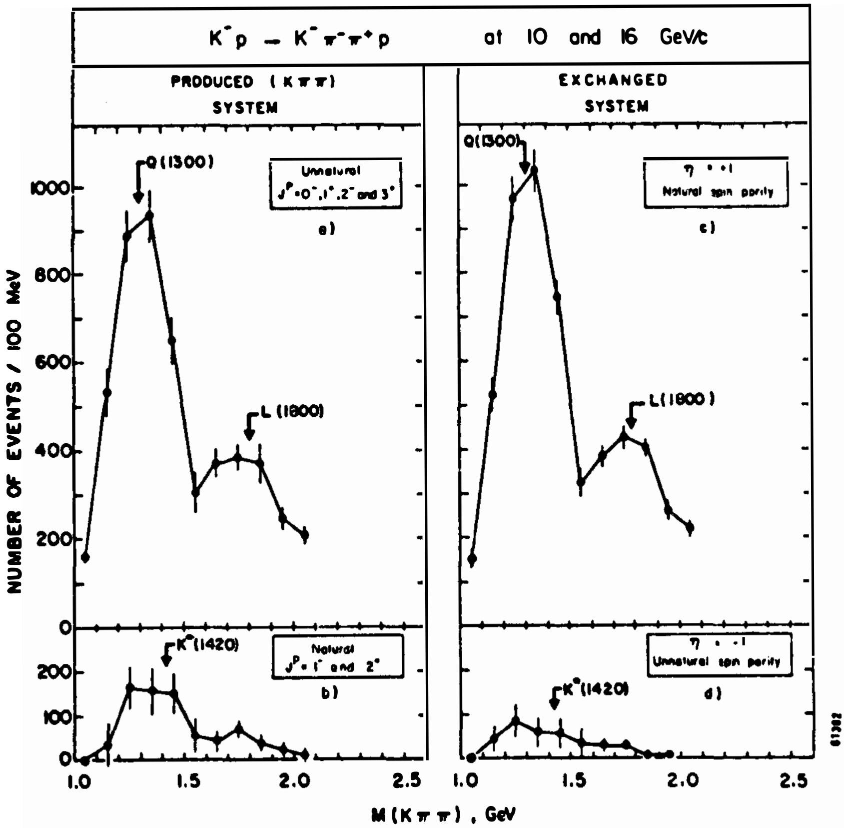

Fig. 1 : In the reaction $K^-p \rightarrow (K^-\pi^+\pi^-)p$ at 10 and 16 GeV/c,
a) and b) : comparison of the number of events having the ($K\pi\pi$) mass system in states of unnatural spin-parity.
c) and d) : comparison of the number of events for which the reaction proceeds via the exchange of natural and of unnatural spin parity [9].

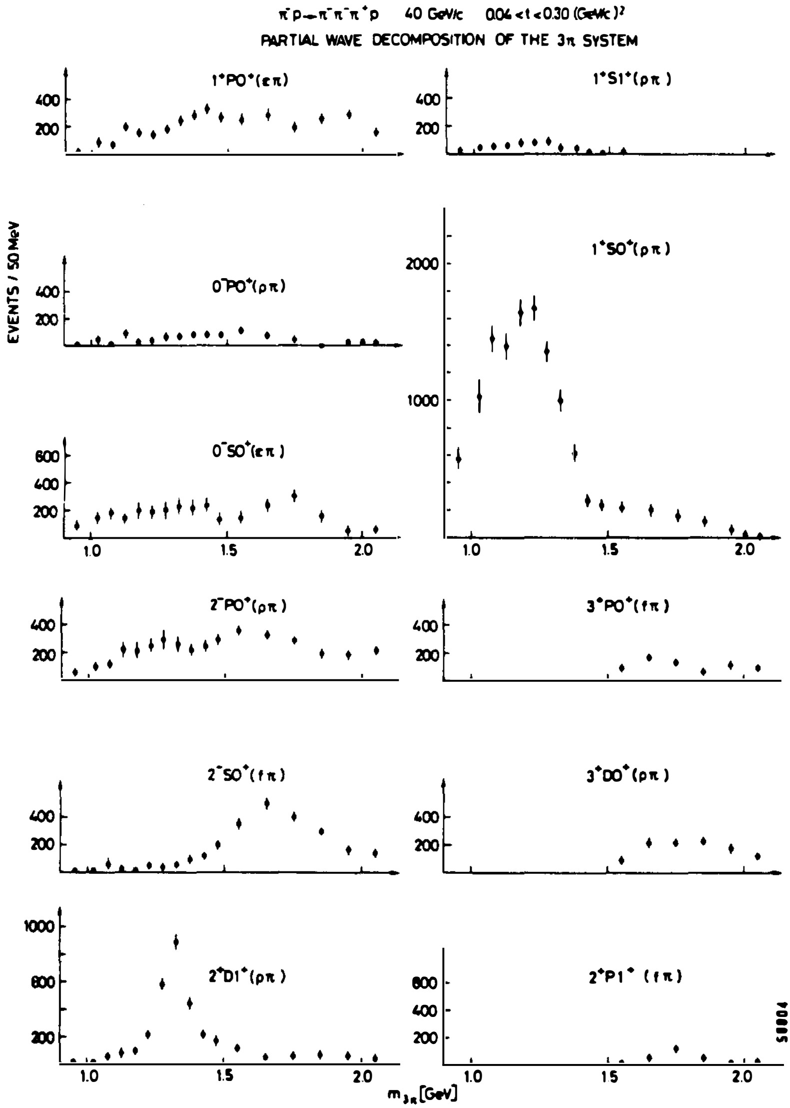

Fig. 2 : Number of events as a function of the (3π) mass obtained from a partial wave decomposition of the (3π) system produced in the reaction $\pi^- p \to (\pi^-\pi^+\pi^-)p$ at 40 GeV/c [7].

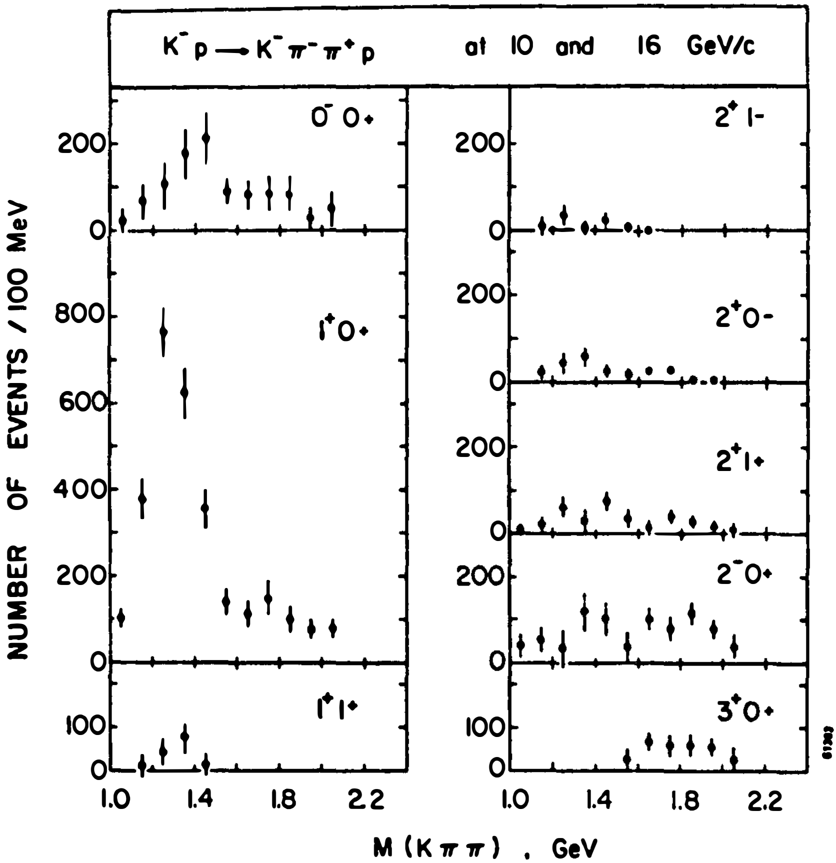

Fig. 3 : Number of events in each $|J^P M\eta>$ state, as a function of the $(K\pi\pi)$ mass produced in the reaction $K^-p \rightarrow (K^-\pi^+\pi^-)p$. J and P are the spin and parity of the $(K\pi\pi)$ system. M is the z- component of angular momentum in the Gottfried-Jackson frame and y is the eigenvalue of the reflection operator in the production plane. For $M = 0$, $\eta = +1$ for natural parity exchange and $\eta = -1$ for unnatural parity exchange [9].

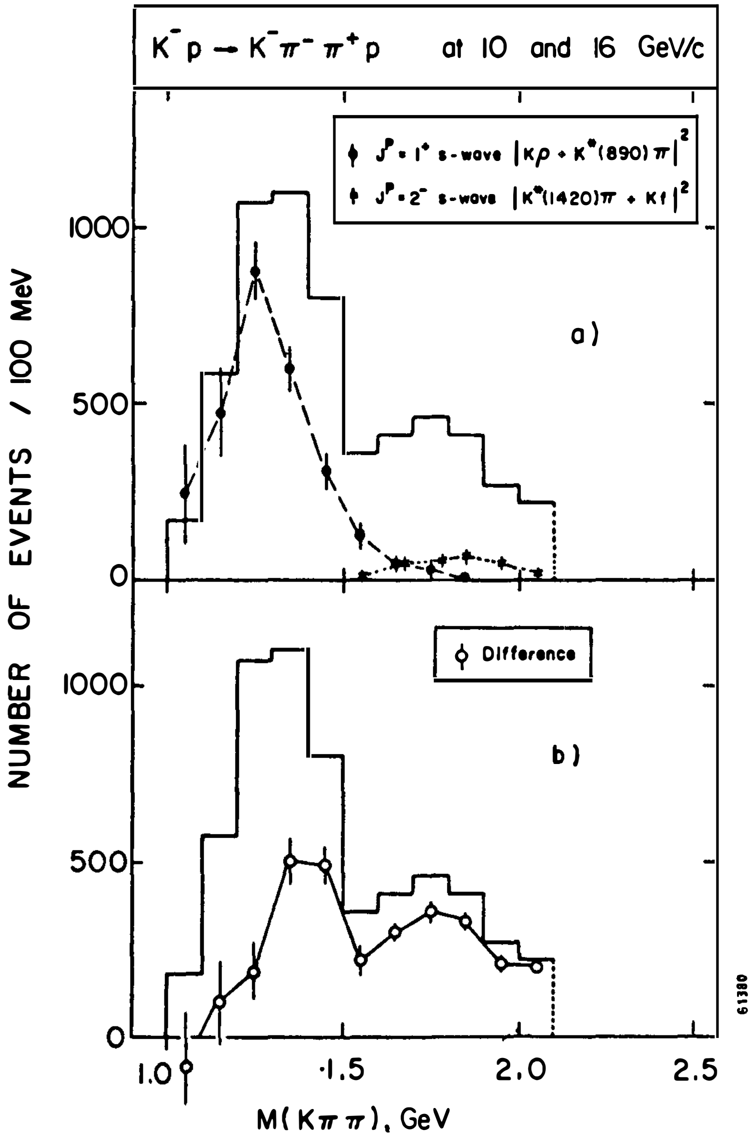

Fig. 4 : a) Comparison of the experimental mass spectrum, corrected for the cuts made in selecting the sample used in the analysis with the contributions of i) the Kρ, $K^*(890)\pi$ and $K\rho/K^*(890)\pi$ interference from the state $J^P = 1^+$ S wave (solid circles) and ii) the $K^*(1420)\pi$, Kf and $K^*(1420)\pi$ /Kf interference from the state $J^P = 2^-$S- wave (crosses).

b) Difference (open circles) between the total mass spectrum and the sum of the two contributions from $J^P = 1^+$ and $J^P = 2^-$ shown separately in a) [9].

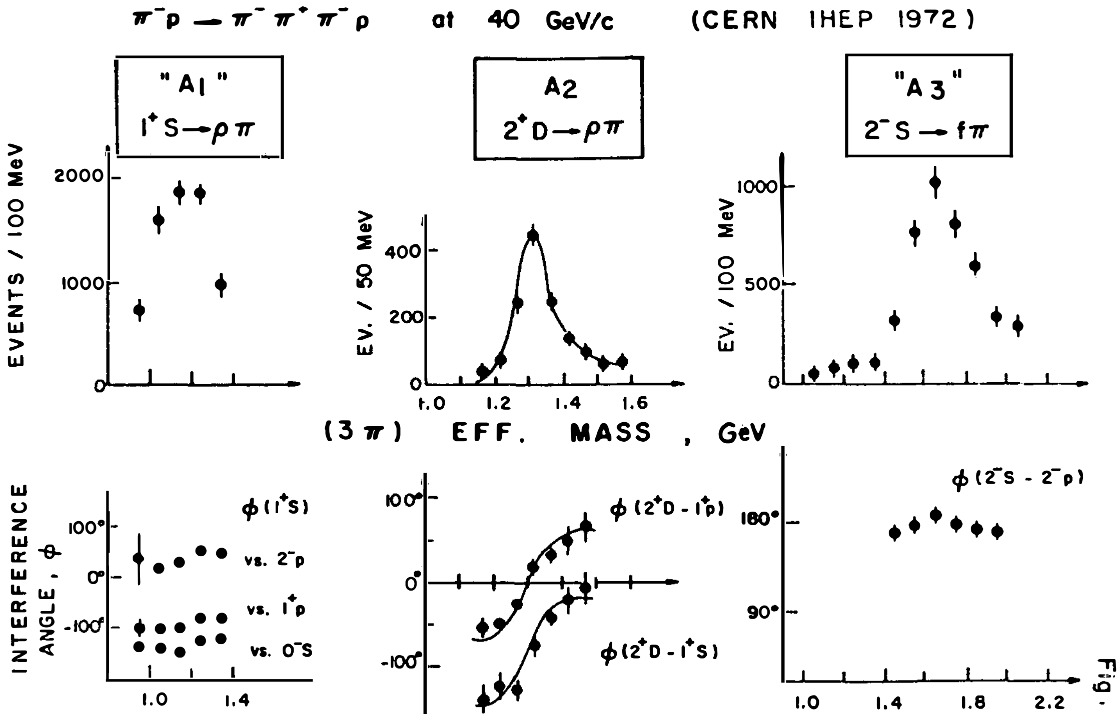

Fig. 5 : For the reaction $\pi^- p \to \pi^-\pi^-\pi^+ p$ at 40 GeV/c, the number of events is plotted as a function of the (3π) mass for the 1^+S- wave decaying into $\rho\pi$ (called A_1) for the 2^+D- wave decaying into $\rho\pi$ (called the A_2) and for the 2^-S- wave decaying into $f\pi$ (called the A_3). Below the relative phase or interference angle Ø, between each of these 3 waves and the background waves indicated, is shown [7].

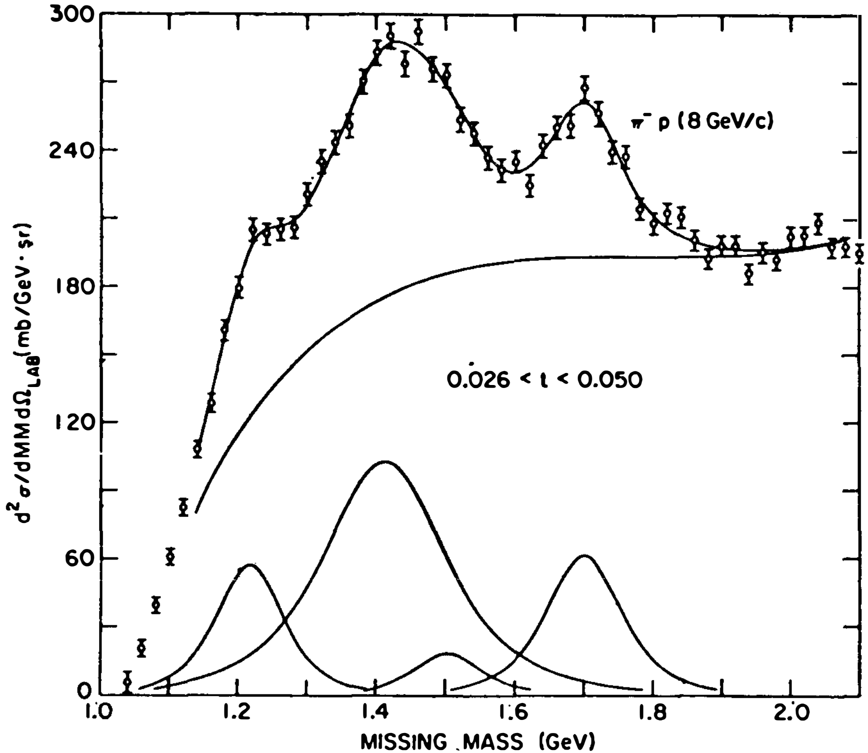

Fig. 6 : Cross section as a function of missing mass for the reaction $\pi^- p \to \pi^-$ + anything, at 8 GeV/c at 0.026 < $|t|$ < 0.050 GeV^2. The assumed resonance contributions and background are shown dotted.

Fig. 6

Fig. 7

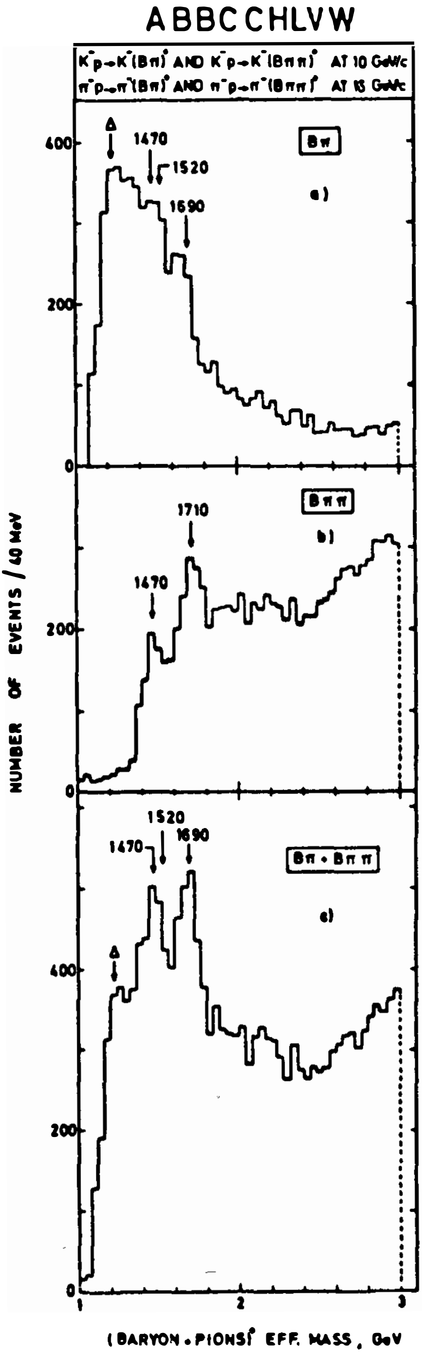
ABBCCHLVW
$K^-p \to K^-(B\pi)^0$ AND $K^-p \to K^-(B\pi\pi)^0$ AT 10 GeV/c
$\pi^-p \to \pi^-(B\pi)^0$ AND $\pi^-p \to \pi^-(B\pi\pi)^0$ AT 15 GeV/c
Bπ
a)
Δ
1470
1520
1690
Bππ
b)
1710
1470
Bπ + Bππ
c)
1520
1470
1690
Δ
400
200
0
1
2
3
NUMBER OF EVENTS / 40 MeV
(BARYON + PIONS)^0 EFF. MASS, GeV

Fig. 11

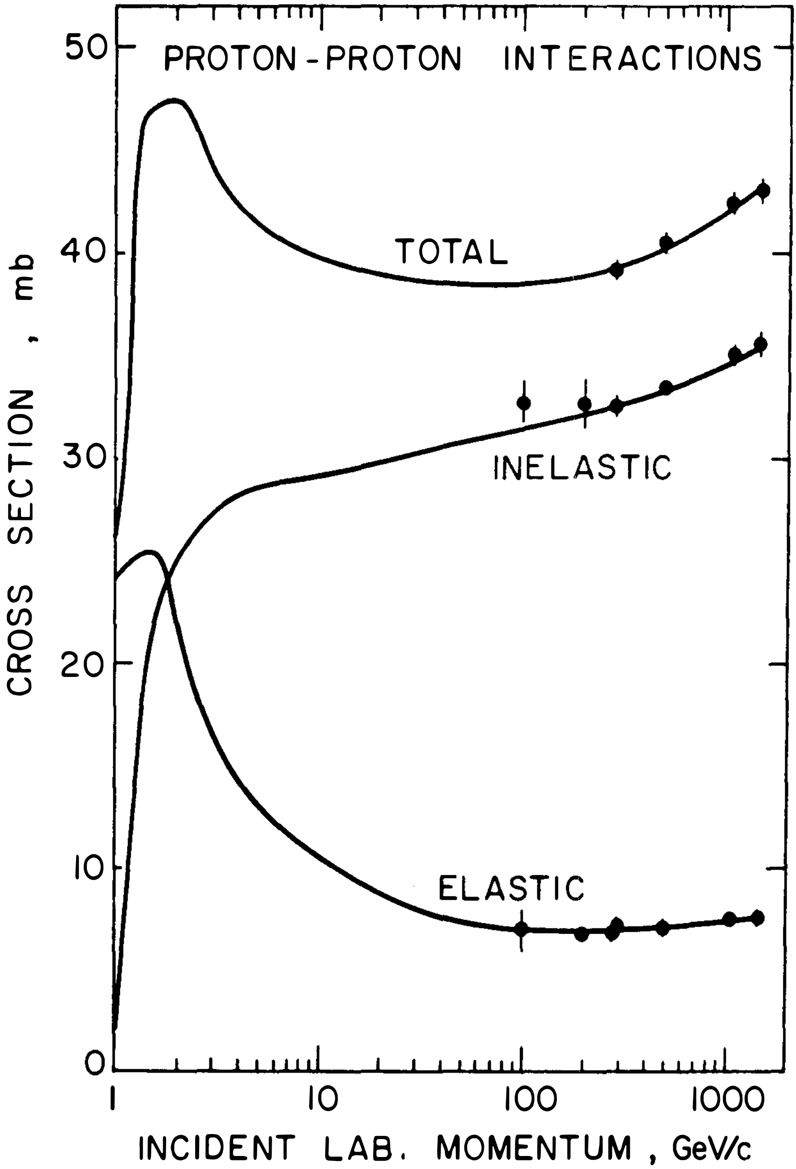

Fig. 11 : Total, elastic and inelastic cross sections for pp reactions as a function of the incident laboratory momentum [13].

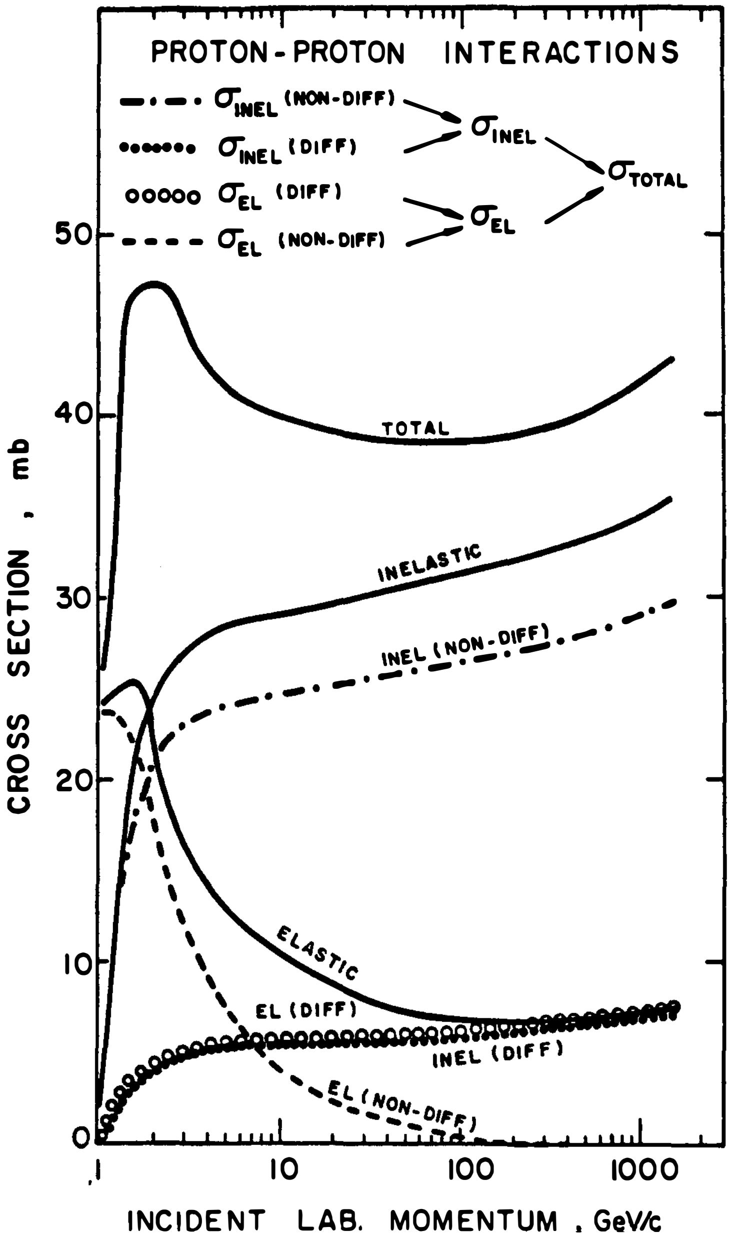

Fig. 13 : Cross section as a function of incident lab. momentum in pp reactions for total, elastic and inelastic reactions (solid lines), for inelastic (non-diffractive) (dot-dash), inelastic (diffractive) (dots), elastic (diffractive)(open circles), and elastic (non-diffractive or Reggeon exchange) (dashed line) [2].